JPEDAV (2005) 26:430-434
DOI: 10.1361/154770305X66475
1547-7037/$19.00 ©ASM International

Analysis of the Formation of Hollow Nanocrystals: Theory and Monte Carlo Simulation

I.V. Belova and G.E. Murch

(Submitted July 15, 2005)

Experiments on the formation of hollow nanocrystals by way of Kirkendall porosity resulting from a vary large Kirkendall effect have been reported recently by Yin et al. (*Science*, Vol 304, 2004, p 711). In the present paper, there is a discussion of some theoretical aspects of this process using chemical diffusion theory in the formal absence of vacancies at equilibrium. A formal description of the observed nanoscale Kirkendall effect is given that accompanies this process. A set of Monte Carlo simulations of the process are performed to verify the theoretical findings.

1. Introduction

Recently, Yin and colleagues at the University of California in Berkeley[1,2] found that when isolated nanocrystals of cobalt are exposed to sulfur at 180 °C, the initially solid nanocrystals quickly turn to hollow spheres of cobalt sulfide. The experiments have been repeated with various other combinations of materials to form nanospheres of cobalt oxide, cobalt selenide, and iron oxide. The nanospheres thus formed are also remarkably uniform: the size of the cavity varies no more than 13% in any given batch. The uniformity and apparent versatility of the nanospheres have suggested a wide range of applications, including drug delivery systems, optics, electronics, and selective chemical reactors, all on the nanoscale. It has even been possible to produce isolated catalyst platinum particles within the hollow shells. It is believed that because the diffusion rate of cobalt is much larger than that of sulfur, during interdiffusion a single large pore forms in the cobalt as a result of Kirkendall porosity.[3]

The usual assumption in analyzing interdiffusion is that vacancy sources and sinks are sufficiently numerous and efficient that the vacancies can be considered always to be at equilibrium. It is known that in general, nanocrystals have a very high degree of perfection with fewer vacancies being present than in micron-sized material. Sources and sinks would have to be at the surfaces of the nanocrystals. The above strongly suggests that the vacancies cannot be considered to be at equilibrium during interdiffusion at the nano level. A similar situation might also reasonably be expected in *any* interdiffusion couple in at least some of the region *between* the sources and sinks of vacancies. Because the theory of interdiffusion under these conditions is rather poorly developed, we have undertaken a general analytical/computer simulation study to explore the phenomenon.

This article is a revised version of the paper printed in the *Proceedings of the First International Conference on Diffusion in Solids and Liquids—DSL-2005*, Aveiro, Portugal, July 6-8, 2005, Andreas Öchsner, José Grácio and Frédéric Barlat, eds., University of Aveiro, 2005.

I.V. Belova and **G.E. Murch,** Diffusion in Solids Group, School of Engineering, The University of Newcastle, Callaghan, New South Wales 2308, Australia. Contact e-mail: Irina.Belova@newcastle.edu.au.

2. Theory

The authors consider an interdiffusion couple prepared as two layers with a total width d of about 100 lattice planes. The internal layer ($\xi_1 \geq \xi \geq \xi_0$) consists of A, which is considered to be a much faster diffuser than the external layer, which is of material B ($\xi_2 \geq \xi \geq \xi_1$, $\xi_2 - \xi_1 = d$). For definiteness, assume that the ratio of exchange frequencies $w_A/w_B = 100$. Also assume that the total vacancy flux through the couple is non-zero because the diffusion couple is moving (growing at external boundary and disappearing at the internal boundary with no vacancy sinks and sources within the diffusion couple) during the interdiffusion process. The overall vacancy concentration is small enough to assume that the atomic fractions $c_A + c_B \approx 1.0$. Two frames of reference are considered (coordinate systems). One is "frozen" into the crystal planes. The other system is a moving coordinate system having a velocity v (in the spherical geometry the velocity v is a function of time and radius).

In the following analysis the authors will not make the usual assumption that the driving force from vacancies is zero. For the fluxes in the lattice frame there are the following Onsager expressions for the fluxes[4]:

$$J_A^0 = L_{AA}(X_A - X_V) + L_{AB}(X_B - X_V)$$
$$J_B^0 = L_{AB}(X_A - X_V) + L_{BB}(X_B - X_V) \quad \text{(Eq 1)}$$

and

$$J_A^0 = c_A N v(r,t) + A(r,t)$$
$$J_B^0 = c_B N v(r,t) - A(r,t) \quad \text{(Eq 2)}$$

where N is the total number of sites per unit volume, the L_{ij} are the Onsager phenomenological coefficients, and the driving forces X_i are given by $-\nabla\mu_i$ and the μ_i, the chemical potentials of species i, are given by $kT \ln c_i$ where c_i is the site fraction of species i (assume ideal mixing of the components). The first terms in Eq 2 are drift terms and are the result of the (total) vacancy flux, and the second terms

are purely "diffusive" contributions to the fluxes. From Eq 2 the vacancy flux is:

$$J_V^0 = (J_A^0 + J_B^0) = -(c_A + c_B)Nv(r,t) \quad \text{(Eq 3)}$$

The fluxes in the moving coordinate system are

$$J_A = A(r,t) \quad J_B = -A(r,t) \quad J_V = Nv(r,t) \quad \text{(Eq 4)}$$

After eliminating the functions $A(r,t)$ and X_V from Eq 1 and 2:

$$J_A^0 = -D_A^I \nabla c_A - L_A X_v = \frac{L_A D_B^I + L_B D_A^I}{L} \nabla c_A + \frac{L_A}{L} Nv$$

$$J_B^0 = -D_B^I \nabla c_A - L_B X_v = \frac{L_A D_B^I + L_B D_A^I}{L} \nabla c_A + \frac{L_B}{L} Nv \quad \text{(Eq 5)}$$

where $L_i = L_{ii} + L_{AB}$ and $L = L_A + L_B$ and, with the usual expressions for the intrinsic diffusion coefficients[4]:

$$D_A^I = \phi kT \left(\frac{L_{AA}}{Nc_A} - \frac{L_{AB}}{Nc_B} \right) \quad D_B^I = \phi kT \left(\frac{L_{BB}}{Nc_B} - \frac{L_{AB}}{Nc_A} \right) \quad \text{(Eq 6)}$$

The expressions Eq 5 and 6 are the most general ones. Note that there is only a restriction on a possible functional form of the velocity v (this form depends on the possible geometry of the diffusion couple: planar, cylindrical, or spherical).

First, apply the Darken formalism[5] to the relations in Eq 5. In the Darken formalism it is assumed that:

$$L_{AA} = \frac{Nc_A D_A^*}{kT} \quad L_{BB} = \frac{Nc_B D_B^*}{kT} \quad L_{AB} = 0 \quad \text{(Eq 7)}$$

where D_A^* and D_B^* are the tracer diffusion coefficients of the species A and B. The fluxes are:

$$J_A^0 = -\frac{D_A^* D_B^* N}{FkT} \phi \nabla c_A + \frac{c_A D_A^*}{F} Nv$$

$$= -\frac{D_A^*}{F} \left(\frac{D_B^* N}{kT} \phi \nabla c_A - c_A Nv \right)$$

$$J_B^0 = \frac{D_A^* D_B^* N}{FkT} \phi \nabla c_A + \frac{c_B D_B^*}{F} Nv$$

$$= \frac{D_B^*}{F} \left(\frac{D_A^* N}{kT} \phi \nabla c_A + c_B Nv \right) \quad \text{(Eq 8)}$$

with the expression for X_V as:

$$X_V = \frac{(D_B^* - D_A^*)N}{kTF} \phi \nabla c_A - \frac{Nv}{F} \quad \text{(Eq 9)}$$

where $F = c_A D_A^* + c_B D_B^*$. From Eq 9 it is clear that when $v \equiv 0$ (and therefore $J_V^0 \equiv 0$) and $\nabla c_A \neq 0$ then $X_V \neq 0$. (This will mean that the vacancy concentration in the couple may not be constant even with a zero vacancy flux.) Conversely, if $X_V = 0$ then $J_V^0 \neq 0$.

Next, we apply the Manning formalism[6,7] and compare the resulting expressions with the Darken expressions in Eq 8 and 9. In the Manning formalism (for the connection between chemical and tracer diffusion coefficients) the relations for the binary system are:

$$L_{AA} = \frac{Nc_A D_A^*}{kT} \left(1 + \frac{2c_A D_A^*}{M_0 F} \right)$$

$$L_{BB} = \frac{Nc_B D_B^*}{kT} \left(1 + \frac{2c_B D_B^*}{M_0 F} \right)$$

$$L_{AB} = \frac{c_A c_B D_A^* D_B^* N}{M_0 FkT} \quad \text{(Eq 10)}$$

where $M_0 = 2f_0/(1 - f_0)$ where f_0 is the geometric tracer correlation factor for the structure.

The application of Eq 10 to Eq 5 gives:

$$J_A^0 = -\frac{D_A^* D_B^* N}{FkT} \phi \nabla c_A + \frac{c_A D_A^*}{F} Nv$$

$$= -\frac{D_A^*}{F} \left(\frac{D_B^* N}{kT} \phi \nabla c_A - c_A Nv \right)$$

$$J_B^0 = \frac{D_A^* D_B^* N}{FkT} \phi \nabla c_A + \frac{c_B D_B^*}{F} Nv$$

$$= \frac{D_B^*}{F} \left(\frac{D_A^* N}{kT} \phi \nabla c_A + c_B Nv \right) \quad \text{(Eq 11)}$$

$$X_V = \frac{(D_B^* - D_A^*)N}{kTF} \phi \nabla c_A - \frac{f_0 Nv}{F} \quad \text{(Eq 12)}$$

Comparing Eq 8 and 11 there is no difference between the applications of the Darken or Manning formalism to the general flux equations describing the interdiffusion experiment. This is a very surprising result. On the other hand, there is (possibly) a significant difference between the expressions for X_V: Eq 9 and 12. For example, with the usually accepted assumption that X_V is equal to 0 for interdiffusion, there is the well-known result:

$$J_A^0 = -D_A^I \nabla c_A \quad J_B^0 = D_B^I \nabla c_A \quad J_V^0 = (D_A^I - D_B^I) \nabla c_A \quad \text{(Eq 13)}$$

These equations contain only intrinsic diffusivities and the difference between them. The Darken formalism gives:

$$D_A^I = D_A^* \phi \quad D_B^I = D_B^* \phi$$

$$D_A^I - D_B^I = (D_A^* - D_B^*) \phi \quad \text{(Darken)} \quad \text{(Eq 14)}$$

whereas the Manning formalism gives:

$$D_A^I = \frac{D_A^*(D_A^*(f_0 - c_B) + c_B D_B^*)}{f_0 F}\phi$$

$$D_B^I = \frac{D_B^*(D_B^*(f_0 - c_A) + c_A D_A^*)}{f_0 F}\phi$$

$$D_A^I - D_B^I = \frac{D_A^* - D_B^*}{f_0}\phi \quad \text{(Manning)} \qquad \text{(Eq 15)}$$

3. Numerical Simulation

The problem of interdiffusion at the nanoscale described above allows for three different geometries: planar, cylindrical, and spherical. The experiments forming hollow nanocrystals were done for spherical geometry.[1,2] Under the assumption that at the initial time $t = 0$ there is no material at $r = 0$ the general behavior of the interdiffusion couple in the spherical geometry can be modeled perfectly by the problem in planar geometry. Because of this, for the purposes of this paper the authors performed numerical simulations in a planar geometry. The velocity $v = v(\xi,t)$ (ξ is the coordinate perpendicular to the interface plane between A and B, $w_A/w_B = 100$, t is time) then becomes a function independent of spatial coordinate ξ: $v = v(t)$. In the numerical algorithm the left boundary of the couple is modeled (slower diffuser end) as an active vacancy source and the right boundary as an active vacancy sink (faster diffuser end). The initial distribution of A and B is $c_A = 1 - c_V$, $c_B = 0$ at $0.5 > \xi \geq 0.1$; and $c_B = 1 - c_V$, $c_A = 0$ at $0.9 \geq \xi \geq 0.5$.

4. Results

Three cases of the boundary conditions were considered for the vacancy concentration. In the first, $c_V(\xi = 0.9,t) = 0.0$; $c_V(\xi = 0.1,t) =$ constant. The results for this case are shown in Fig. 1 and 2. There is no movement of the specimen in this case because of the superimposed vacancy gradient working against it. Therefore $J_V^0 = 0$ and the atomic concentrations are "symmetric." As time progresses the vacancy and atoms gradually become distributed homogenously through the diffusion couple.

In the second case $c_V(\xi = 0.9, t) = c_V(\xi = 0.1,t) =$ constant. The results for this case are shown in Fig. 3 and 4. During interdiffusion, the diffusion couple moves some 25% of its length, creating further porosity. Anomalous behavior (compared with standard interdiffusion couples) of the atomic and vacancy profiles occurs because there are no active vacancy sources and sinks within the diffusion zone. At short times, vacancies are depleted quickly on the slow diffuser side. Continued depletion occurs before the couple starts moving (top part of Fig. 4). Once the vacancies are taken directly from the left boundary (modeled as an active source of vacancies in the computer simulation), the movement of the couple starts. At the same time, the interdiffusion process proceeds in the usual way (the top part of Fig. 3 shows symmetric atomic concentration profiles). Once movement starts, the interdiffusion process is somewhat accelerated (middle parts of Fig. 3 and 4). At some stage there is no need for vacancy depletion any longer, and the active sink (right boundary) stops, but the active source is still in operation until both the vacancy and atomic concentrations become constant across the sample (end of interdiffusion process: bottom parts of Fig. 3 and 4).

In the third case, $c_V(\xi = 0.9,t) =$ constant; $c_V(\xi = 0.1,t) = 0.0$. The results for this case are shown in Fig. 5 and 6.

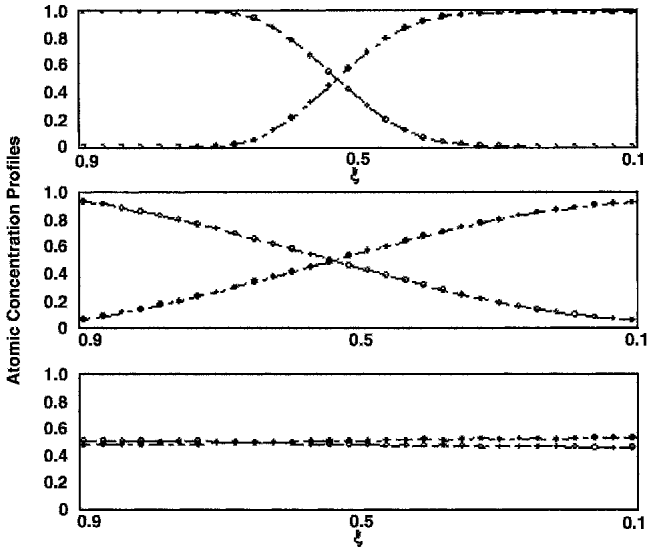

Fig. 1 Results of the numerical simulation of the interdiffusion problem with the first combination of the vacancy boundary conditions after time t, $10t$, and $100t$ (starting from the top). ●: concentration of the faster A atomic component; ○: concentration of the slower B atomic component

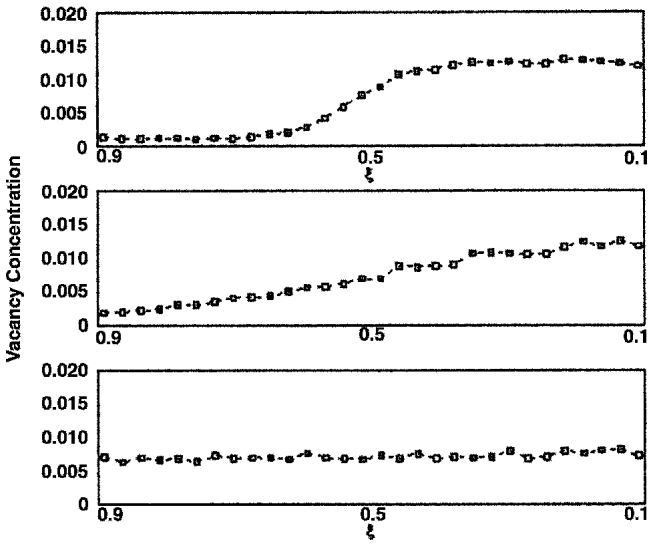

Fig. 2 Results of the numerical simulation of the interdiffusion problem with the first combination of the vacancy boundary conditions after time t, $10t$, and $100t$ (starting from the top). □: vacancy concentration distribution

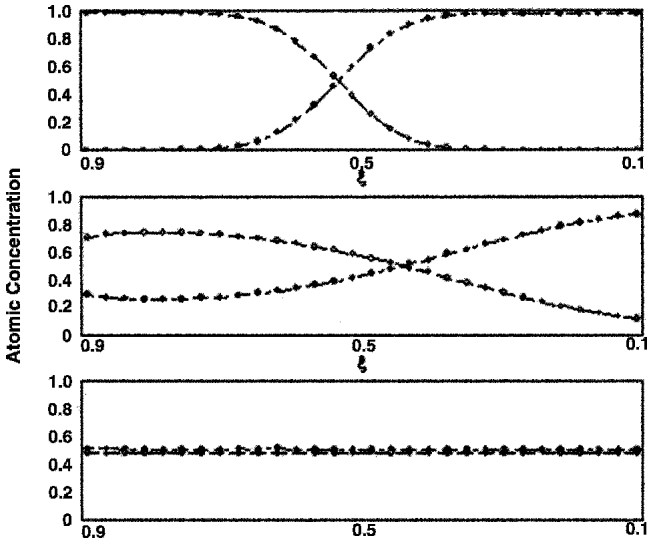

Fig. 3 Results of the numerical simulation of the interdiffusion problem with the second combination of the vacancy boundary conditions after time t, $10t$, and $100t$ (starting from the top). ●: concentration of the faster A atomic component; ○: concentration of the slower B

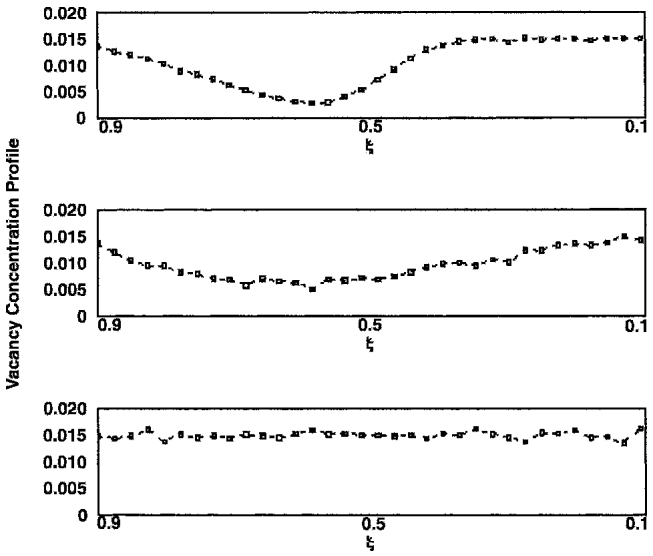

Fig. 4 Results of numerical simulation of the interdiffusion problem with the second combination of the vacancy boundary conditions after time t, $10t$, and $100t$ (starting from the top). □: vacancy concentration distribution

In this case, the rate of total interdiffusion is enhanced greatly by the vacancy gradient. The vacancy gradient produces a movement of the specimen because of a corresponding segregation or demixing. That is exactly what seems to be happening at advanced stages of the process. For planar geometry, this case allows for a steady state to be reached. Cylindrical and spherical geometries for this case must have a "final" stage of interdiffusion-segregation process at which the internal and external radii reach their maxima and the width d its minimum.

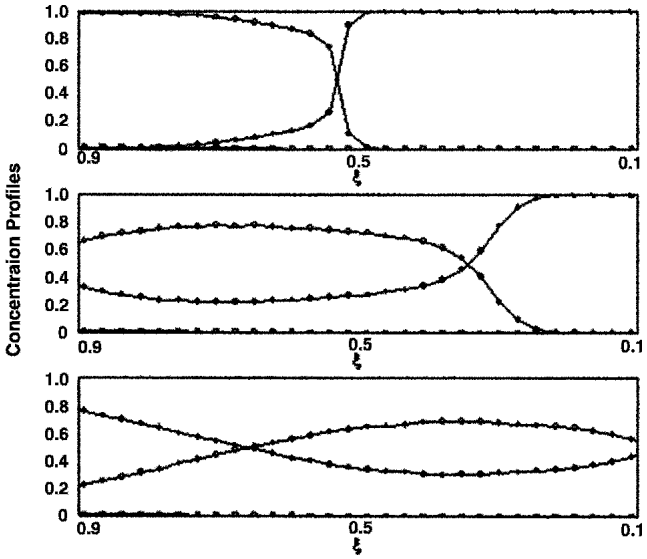

Fig. 5 Results of the numerical simulation of the interdiffusion problem with the third combination of the vacancy boundary conditions after time t, $10t$, and $100t$ (starting from the top). ●: concentration of the faster A atomic component; ○: concentration of the slower B

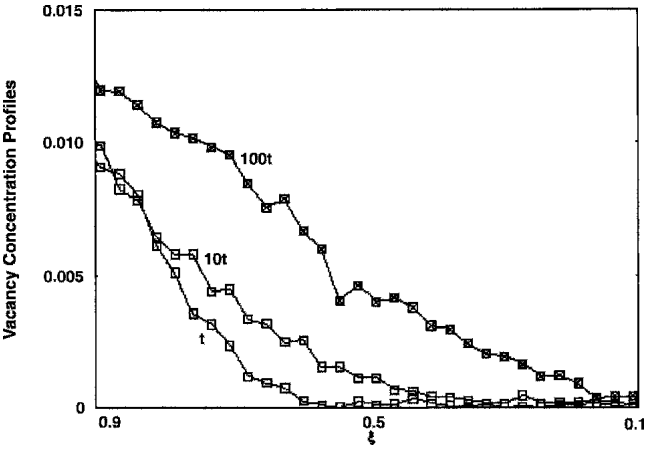

Fig. 6 Results of the numerical simulation of the interdiffusion problem with the third combination of the vacancy boundary conditions after time t, $10t$, and $100t$. □: vacancy concentration

5. Conclusions

Experiments on the formation of hollow nanocrystals by way of Kirkendall porosity resulting from a large Kirkendall effect have been reported recently by Yin et al.[1,2] In the present paper, we have developed a description of interdiffusion in a binary interdiffusion couple in the formal absence of vacancies at equilibrium. A formal description of the observed nanoscale Kirkendall effect is given that accompanies this process. A set of Monte Carlo computer simulations of the process were performed to explore the theoretical/experimental findings.

Acknowledgments

This work was supported by the Australian Research Council (Discovery Project Grants Scheme) and an Australian Research Council Australian professorial fellowship (to I.V.B).

References

1. Y. Yin, R. Rioux, C.K. Erdonmez, S. Hughes, G.A. Somorjai, and A.P. Alivisatos, Formation of Hollow Nanocrystals through the Nanoscale Kirkendall Effect, *Science,* Vol 304, 2004, p 711
2. Y. Yin and A.P. Alivisatos, "Synthesis of Hollow Cobalt Chalcogenides Nanostructures," paper M5.43 presented at the Materials Research Society Spring Meeting (San Francisco), 2004
3. A.D. Smigelskas and E.O. Kirkendall, Zinc Diffusion in Alpha Brass, *Trans. AIME,* Vol 171, 1947, p 130
4. J. Philibert, *Atom Movements*: *Diffusion and Mass Transport in Solids,* Editions de Physique, Les Ulis, 1991
5. L.S. Darken, Diffusion, Mobility and Their Interrelation through Free Energy in Binary Metallic Systems, *Trans. Am. Inst. Min.* (*Metall.*) *Eng.,* Vol 175, 1948, p 184
6. J.R. Manning, Correlation Factors for Diffusion in Nondilute Alloys, *Phys. Rev. B,* Vol 4, 1971, p 1111
7. J.R. Manning, *Diffusion Kinetics for Atoms in Crystals,* Van Nostrand, Princeton, NJ, 1968